catalysts

MDPI

Supplementary Materials

Effective Glycosylation of Cucurbitacin Mediated by UDP-Glycosyltransferase UGT74AC1 and Molecular Dynamics Exploration of Its Substrate Binding Conformations

Shicheng Mu, Jiao Li, Cui Liu, Yan Zeng, Yan Men, Yi Cai, Ning Chen, Hongwu Ma and Yuanxia Sun*

Table of contents

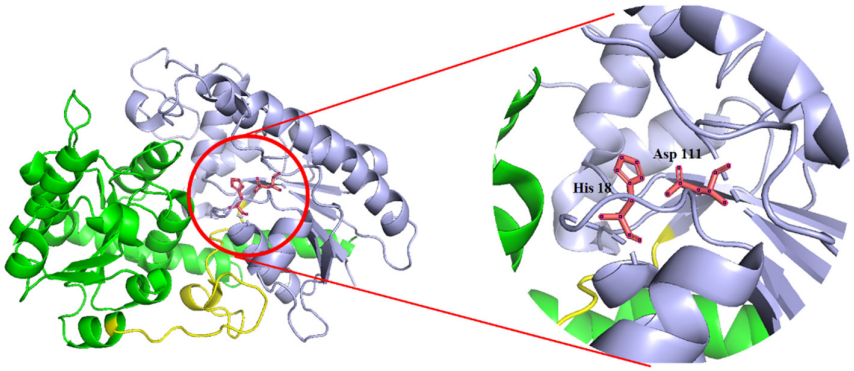

Figure S1. Crystal structures of UGT74AC1. The secondary structures within N-domain (Met1-Lys226) and C-domain (Cys259-Thr454) are colored purple and green, respectively. The linker between C-domain and N-domain from residues Thr227-Val258 is colored yellow. A detailed active site view of UGT74AC1 is on the right. The catalytic residues His18 and Asp111 are shown as red sticks.

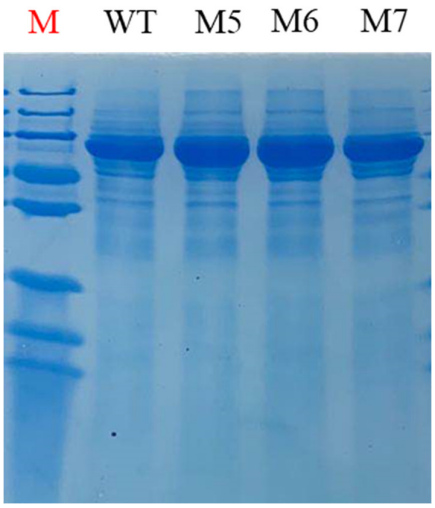

Figure S2. SDS-PAGE of recombinant UGT74AC1 and its mutants (M5-M7) protein purification fractions. Lane M: the protein molecular weight standard. M5 (GT-SM): T79Y/L48M/R28H/L109I/S15A; M6: T79Y/L48M/R28H/L109I/S15A/M76L; M7: T79Y/L48M/R28H/L109I/S15A/M76L/H47R.

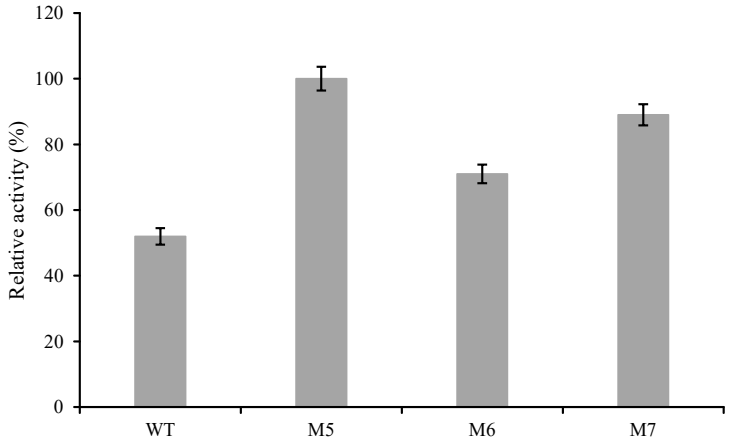

Figure S3. Relative activity of UGT74AC1 and its mutants towards cucurbitacin F 25-acetate.

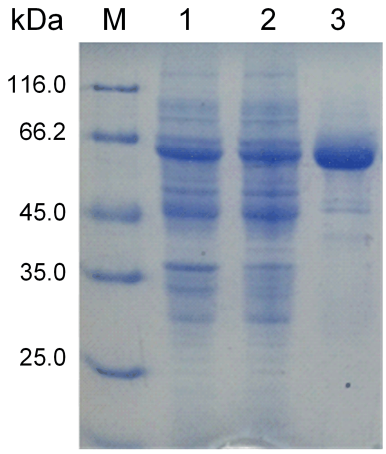

Figure S4. SDS-PAGE of recombinant GT-SM protein fractions. Lane M: the protein molecular weight standard; Lanes 1–3: lysate, supernatant, and purified protein of GT-SM.

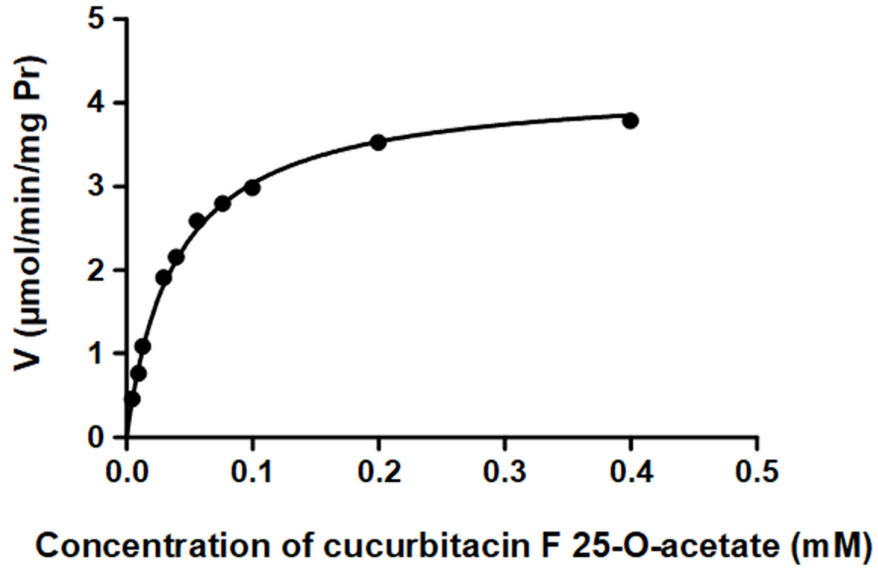

Figure S5. Determination of kinetic parameters for GT-SM on cucurbitacin F 25-acetate.

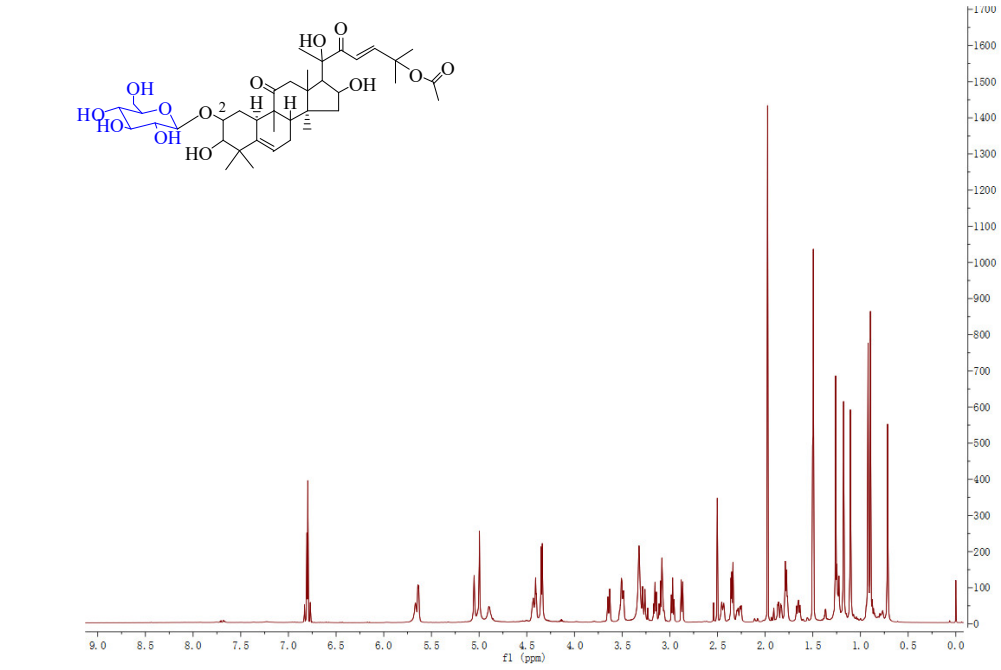

Figure S6. [1]H NMR spectrum of product in dimethyl sulfoxide-d6 (600 MHz).

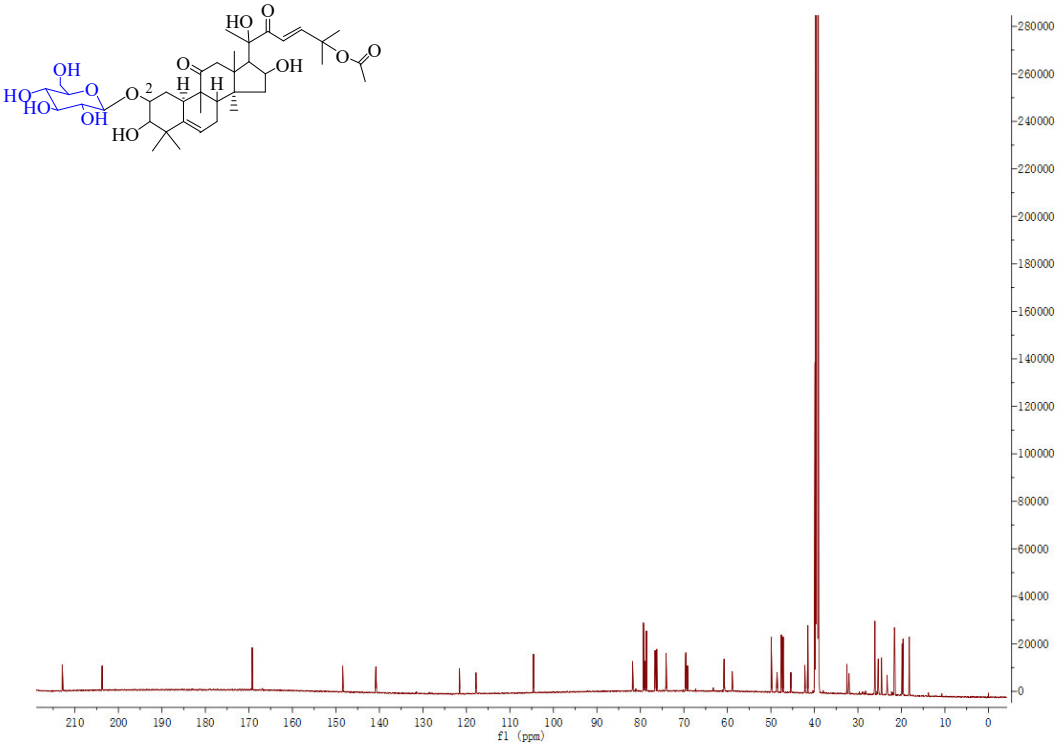

Figure S7. [13]C NMR spectrum of product in dimethyl sulfoxide-d6 (600 MHz).

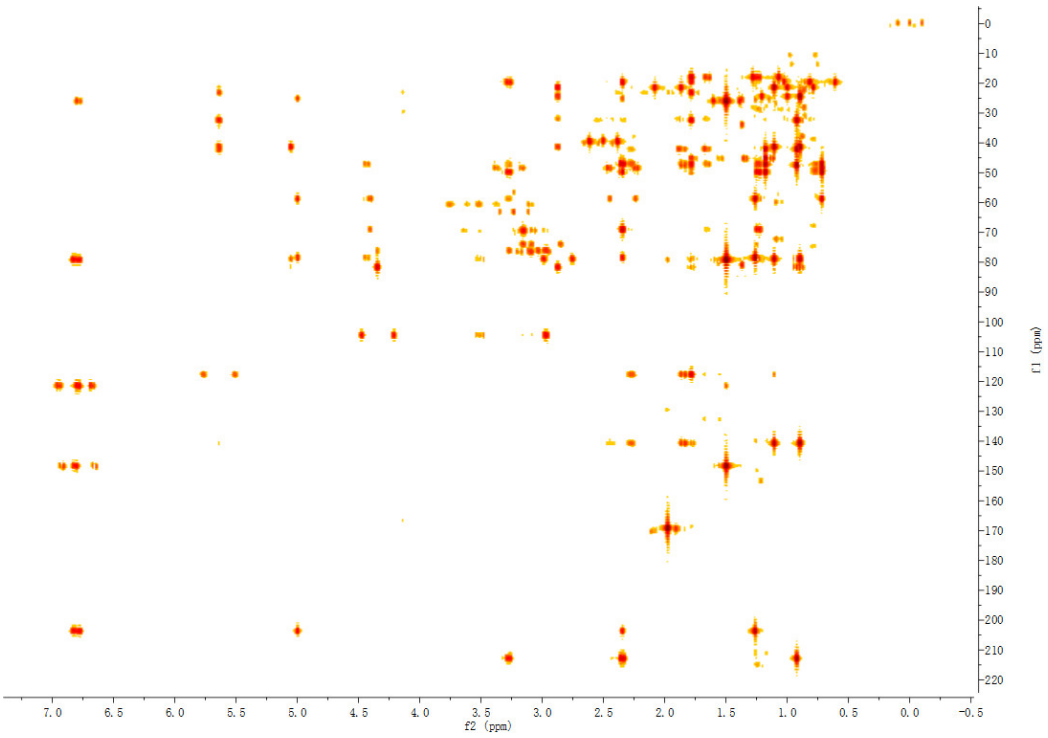

Figure S8. HMBC spectrum of product in dimethyl sulfoxide-d6 (600 MHz).

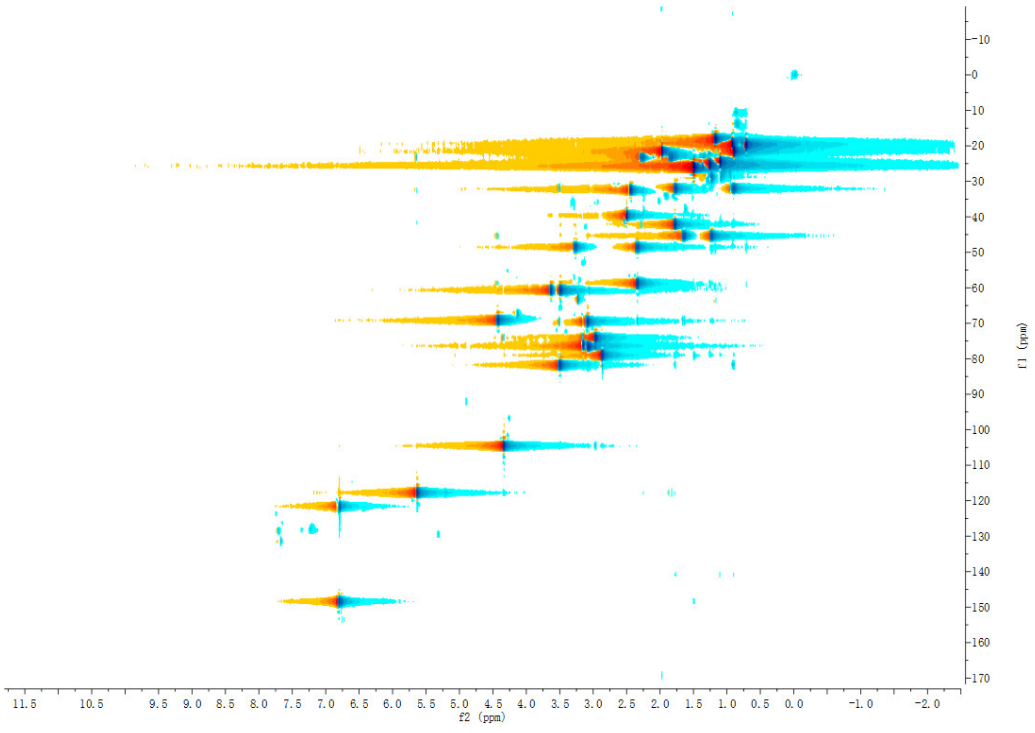

Figure S9. HSQC spectrum of product in dimethyl sulfoxide-d_6 (600 MHz).

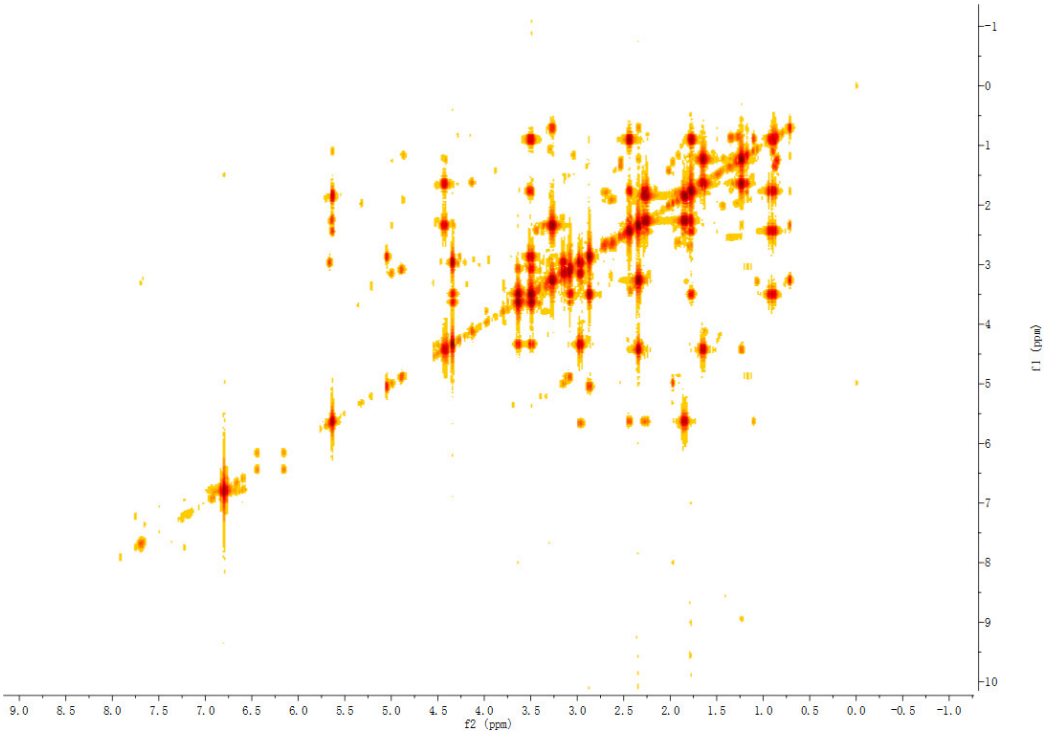

Figure S10. COSY spectrum of product in dimethyl sulfoxide-d_6 (600 MHz).

Supporting method

Modelling and molecular dynamics simulations

The Glide module in Schrödinger program was used to perform molecular docking studies [1]. The GT-SM structure was prepared and then used to build the energy grid. The docking box was set to the binding pocket and its outer box size was set to 28.5*28.5*28.5 Å. The scaling factor for van der Waals radii was set to 1.0 and the XP (extra precision) mode was used. The top-ranked molecules were further selected according to catalytic mechanism. Amber18 molecular dynamics package [2] was used to carry out MD simulation of the selected complex using ff14SB force field for protein [3] and general AMBER force field (GAFF) for substrates. [4] The antechamber module and GAFF2 with AM1-BCC charges are used to obtain force field parameters for substrates [5]. Initially, energy minimization involves 2000 steps steepest descent algorithm followed by 1000 steps of conjugated gradient algorithm was performed for the water and ions, then the entire system. Then, the system was slowly heated up to 300 K and well equilibrated. After that, a 10 ns MD simulation with a distance constraint (3.0 Å, 50 kcal/mol) between the coordinating NE2 atom of catalytic residue His18 and O2 or O3 atom of CA-F25 was carried out to simulate the induced-fit process of substrate binding. Finally, 200ns unconstrained production simulation was performed at 300 K and 1 atm with 2 fs integration time step. The last 100 ns MD trajectories with 10,000 frames in total was used to calculate the emerging frequency of catalytic conformations which was defined according to the reaction mechanism [6]. Periodic boundary condition was implemented using a rectangular TIP3P water box with a buffer distance of 10 Å [7]. During the dynamics, all the bonds involving hydrogen atoms are restrained using the SHAKE algorithm. [8] Particle mesh Ewald (PME) method [9] was applied to account for the long range part of the electrostatic interactions. CPPTRAJ tool was employed to perform various analyses on the MD trajectories [10].

References

1. Glide, Schrödinger, LLC, New York, NY, 2017.
2. D.A. Case, I.Y. Ben-Shalom, S.R. Brozell, D.S. Cerutti, T.E. Cheatham, III, V.W.D. Cruzeiro, T.A. Darden, R.E. Duke, D. Ghoreishi, M.K. Gilson, H. Gohlke, A.W. Goetz, D. Greene, R Harris, N. Homeyer, Y. Huang, S. Izadi, A. Kovalenko, T. Kurtzman, T.S. Lee, S. LeGrand, P. Li, C. Lin, J. Liu, T. Luchko, R. Luo, D.J. Mermelstein, K.M. Merz, Y. Miao, G. Monard, C. Nguyen, H. Nguyen, I. Omelyan, A. Onufriev, F. Pan, R. Qi, D.R. Roe, A. Roitberg, C. Sagui, S. Schott-Verdugo, J. Shen, C.L. Simmerling, J. Smith, R. SalomonFerrer, J. Swails, R.C. Walker, J. Wang, H. Wei, R.M. Wolf, X. Wu, L. Xiao, D.M. York and P.A. Kollman (2018), AMBER 2018, University of California, San Francisco.
3. Maier, J. A.; Martinez, C.; Kasavajhala, K.; Wickstrom, L.; Hauser, K. E.; Simmerling, C. ff14SB: improving the accuracy of protein side chain and backbone parameters from ff99SB. J. Chem. Theory Comput. **2015**, *11*, 3696–3713.
4. Wang, J.; Wolf, R. M.; Caldwell, J. W.; Kollman, P. A.; Case, D. A. Development and Testing of a General Amber Force Field. J. Comput. Chem. **2004**, *25*, 1157–1174.
5. Jakalian, A.; Bush, B. L.; Jack, D. B.; Bayly, C. I. Fast, efficient generation of high-quality atomic charges. AM1-BCC model: I. Method. J. Comput. Chem. **2000**, *21*, 132–146.
6. Nidetzky, B.; Gutmann, A.; Zhong, C. Leloir Glycosyltransferases as Biocatalysts for Chemical Production. ACS Catal. **2018**, *8*, 6283–6300.
7. Jorgensen, W. L.; Chandrasekhar, J.; Madura, J. D.; Impey, R. W.; Klein, M. L.
8. J. Chem. Phys. **1983**, *79*, 926–935.
9. Ryckaert, J. P.; Ciccotti, G.; Berendsen, H. J. Numerical Integration of the Cartesian Equations of Motion of a System with Constraints: Molecular Dynamics of n-alkanes. J. Comput. Phys. **1977**, *23*, 327–341.
10. Essmann, U.; Perera, L.; Berkowitz, M. L.; Darden, T.; Lee, H.; Pedersen, L. G. A Smooth Particle Mesh Ewald Method. The Journal of chemical physics. **1995**, *103*, 8577–8593
11. Roe, D. R.; Cheatham, T. E., III. J. Chem. Theory Comput. **2013**, *9*, 3084–3095.